

# Cysteine residues 87 and 320 in the amino terminal domain of NMDA receptor GluN2A govern its homodimerization but do not influence GluN2A/GluN1 heteromeric assembly

Xiao-Min Zhang, Xin-You Lv, Yang Tang, Li-Jun Zhu, Jian-Hong Luo

*Department of Neurobiology, Key Laboratory of Medical Neurobiology of the Ministry of Health of China, Zhejiang Province  
Key Laboratory of Neurobiology, Zhejiang University School of Medicine, Hangzhou 310058, China*

Corresponding author: Jian-Hong Luo. E-mail: [luojianhong@zju.edu.cn](mailto:luojianhong@zju.edu.cn)

© Shanghai Institutes for Biological Sciences, CAS and Springer-Verlag Berlin Heidelberg 2013

## ABSTRACT

N-Methyl-*D*-aspartate receptors (NMDARs) play a central role in various physiological and pathological processes in the central nervous system. And they are commonly composed of four subunits, two GluN1 subunits and two GluN2 or GluN3 subunits. The different subunit compositions make NMDARs a heterogeneous population with distinct electrophysiological and pharmacological properties and thus with different abilities to conduct neuronal activities. The subunit composition, assembly process, and final structure of assembled NMDARs have been studied for years but no consensus has been achieved. In this study, we investigated the role of the amino terminal domain (ATD) of GluN2A in regulating NMDAR assembly. The ATD of GluN2A was first expressed in heterogeneous cells and the homodimer formation was investigated by fluorescent resonance energy transfer and non-reducing SDS-PAGE electrophoresis. Each of the three cysteine residues located in the ATD was mutated into alanine, and the homodimerization of the ATD or GluN2A, as well as the heteromeric assembly of NMDARs was assessed by non-reducing SDS-PAGE electrophoresis, co-immunoprecipitation and immunocytochemistry. We found that two cysteine residues, C87 and C320, in the ATD of the GluN2A subunit were required for the formation of disulfide bonds and GluN2A ATD homodimers. Furthermore,

the disruption of GluN2A ATD domain dimerization had no influence on the assembly and surface expression of NMDARs. These results suggest that the two ATD domains of GluN2A are structurally adjacent in fully-assembled NMDARs. However, unlike GluN1, the homomerization of the ATD domain of GluN2A is not required for the assembly of NMDARs, implying that GluN2A and GluN1 play unequal roles in NMDAR assembly.

**Keywords:** N-methyl-*D*-aspartate receptor; amino terminal domain; homodimerization; heteromeric assembly

## INTRODUCTION

The N-methyl-*D*-aspartate receptor (NMDAR) is one of the most important ionotropic glutamate receptors in the central nervous system, and plays a major role in various physiological and pathological neuronal processes. Like other ionotropic receptors, NMDARs are tetramers, composed of two obligatory GluN1 subunits and two regulatory GluN2 or GluN3 subunits<sup>[1,2]</sup>. The specific properties of each subunit as well as their assembly in multiple combinations allow NMDARs to establish different neuronal signaling pathways and participate in the regulation of complex functions in the central nervous system. All NMDAR subunits share the same topological structure: an extracellular N-terminus consisting of an amino terminal domain (ATD) and an S1 domain, followed

by three transmembrane regions M1, M3, M4, a re-entrant membrane region (M2) and a loop (S2) between M3 and M4 which forms the ligand-binding domain together with S1, and an intracellular C-terminus which is coupled to downstream signaling pathways.

It is currently believed that the assembly of NMDAR subunits resembles that of the  $\alpha$ -amino-3-hydroxy-5-methyl-4-isoxazolepropionic acid receptor (AMPA), a two-step process which begins with the dimerization of two single subunits, followed by the dimerization of two dimers to form a tetramer. New efforts have been made to elucidate the subunit arrangement in the NMDAR subunit dimers, but the results are controversial. Stoichiometric studies of NMDARs by truncations support the 1-1-2-2 assembly mode, in which GluN1 and GluN2 each assemble into homodimers before further assembling into tetramers<sup>[3]</sup>. Fluorescent resonance energy transfer (FRET) analysis of fluorescence-tagged NMDAR subunits also suggests that GluN1, GluN2A and GluN2B form homodimers in heterogeneous expression systems<sup>[4]</sup>. And it has been reported that GluN1 dimerization is mediated by disulfide bonds with cysteine residue 79 identified as the key residue for the covalent binding of two subunits<sup>[5]</sup>. However, other evidence favors the hypothesis that NMDAR subunits assemble into heterodimers first and two heterodimers further dimerize into tetramers. The ATD and the linker domain between M3 and S2 of GluN1 and GluN2A form heterodimers by covalent bonds if the amino-acids at specific sites are mutated to cysteine<sup>[6,7]</sup>. The crystal structures of the ligand-binding core of GluN2A with glutamate and that of the GluN1-GluN2A heterodimer with glutamate and glycine have been investigated, and the electrophysiological results further confirmed that GluN1-GluN2A heterodimer could be the functional unit of assembled NMDARs<sup>[8]</sup>.

Although the specific process of NMDAR assembly is unclear, the AMPAR with similar structural properties is relatively much better understood. The homodimerization of the AMPAR ATD is believed to initiate AMPAR assembly, and the kainate receptor ATD may serve the same purpose<sup>[9]</sup>. But NMDAR subunits lacking the ATD can still assemble into intact and functional receptors<sup>[10]</sup>. And the NMDAR transmembrane domain may undergo self-assembly, pointing to a novel assembly mode mediated by the transmembrane region, and this differs from AMPARs<sup>[11]</sup>.

Nevertheless, in these experiments, subunit deletion mutations were used. Studies on full-length GluN1 subunits indicate that the ATD-mediated dimerization is cysteine-dependent, which is important for the further assembly of NMDARs<sup>[5]</sup>. So whether NMDAR assembly is initiated by the ATD, as in AMPARs, remains in question.

Revealing the assembly mode of NMDAR subunits can promote further understanding of how different combinations of NMDAR subunits are elaborately regulated in time and space. In this study, we investigated whether dimerization of the GluN2A ATD marks the beginning of NMDAR assembly.

## MATERIALS AND METHODS

### Plasmid Construction

pD-CFP/YFP was constructed by attaching CFP or YFP into the p-Display plasmid between the XmaI and SacII restriction endonuclease sites. And the ATD of GluN2A was then inserted between CFP/YFP and the transmembrane region of p-Display at Sall restriction endonuclease sites to obtain pD-ATD<sub>2A</sub>-CFP/YFP. The plasmid pD-ATD<sub>GluN1</sub> was constructed by inserting the ATD of GluN1 between the leading sequence and the transmembrane domain encoded by the p-Display plasmid using the restriction endonuclease site of Sall. The GluN1-ATD comprises the first 390 amino-acids following the signal peptide of GluN1, and the GluN2A-ATD comprises the first 391 amino-acids following the signal peptide of GluN2A. GluN2A-CFP was constructed as previously described<sup>[4]</sup>. CFP was inserted into GluN2A between the signal peptide and the ATD, making use of a SacII restriction endonuclease site created by site-directed mutation.

The site-directed mutation of pD-ATD<sub>2A</sub>-CFP and GluN2A-CFP was performed using PfuUltra II Fusion HS DNA polymerase (Agilent Technologies, Santa Clara, CA) and PrimeSTAR HS DNA polymerase (Takara, Otsu, Japan), respectively, with complementary primers. The primers were as follows: C87A forward: (5'-3') CTCATCACGCATGTGGCCGACCTCATGTCCGGG, retro-forward: (5'-3') CCCGGACATGAGTCCGCCACATGCGTGATGAG; C231A forward: (5'-3') GTCATCCTGCTCTACGCCTCCAAAGACGAGGCT, retro-forward: (5'-3') AGCCTCGTCTTTGGAGGCGTAGAGCAGGATGAC;

C320A forward: (5'-3') GAGGCCAAGGCCAGCGCCTA-TGGGCAGGCAGAG, retro-forward: (5'-3') CTCTGCCTG-CCCATAGGCGCTGGCCTTGGCCTC.

### Cell Culture and Transfection

HEK293 and COS-7 cells were cultured in Dulbecco's modified Eagle's medium supplemented with 10% fetal bovine serum and antibiotics (Invitrogen, Grand Island, NY). Cells were plated on coverslips or in dishes 24 h before transfection. Lipofectamine 2000 (Invitrogen, Grand Island, NY) was used with the appropriate proportion of plasmids (2 µg each for 35-mm dishes, and 4 µg each for 60-mm dishes) according to the manufacturer's protocol. The transfection mixture was replaced with fresh culture medium after 3 h. For the GluN2A and GluN1 co-transfected group, the culture medium contained D-APV (40 µmol/L, Sigma) to protect the cells from NMDAR-mediated toxicity. Twenty-four hours after transfection, the cells were fixed for staining or harvested for Western blot.

Cortical neuronal cultures were prepared following the protocol described previously<sup>[12]</sup>. Neurons were transfected at 10 days *in vitro*, using Lipofectamine LTX with PLUS (Invitrogen). The transfection mixture was replaced by culture medium that had been collected before transfection. Two micrograms of plasmids for 35-mm dishes were used according to the manufacturer's protocol. After 4 days in culture, the neurons were fixed for staining.

### Immunocytochemistry

The methods of surface immunostaining have been described previously<sup>[12,13]</sup> except for some minor modifications. Briefly, the transfected COS-7 cells or cortical neurons were rinsed twice in extracellular solution, incubated with 0.5% BSA in extracellular solution for 10 min to block nonspecific binding of the antibodies, incubated with rabbit anti-GFP antibody (Abcam, ab290) for 10 min, and rinsed three times. The Alexa546-conjugated donkey anti-rabbit secondary antibody (Invitrogen) was applied for another 10 min. To amplify the fluorescent signal of CFP attached to chimera proteins, the cells were then fixed, permeabilized, and stained again with rabbit anti-GFP antibody for 1 h, followed by Alexa488-conjugated secondary antibody (Invitrogen) for 1 h to mark the total expression of CFP-tagged protein in transfected cells. Finally, the cells were examined under a 60×, 1.7 numerical

aperture oil-immersion objective on a confocal microscope (Olympus, Japan).

In the subcellular localization experiment, the transfected COS-7 cells were fixed in 4% paraformaldehyde for 10 min, followed by blocking and permeabilization in PBS containing 0.1% Triton and 2.5% BSA. Then cells were stained in PBS containing both rabbit anti-GFP (Abcam, ab290) and mouse anti-calreticulin (Abcam, ab22683) for 1 h, rinsed three times in PBS, and finally examined under the confocal microscope.

### Western Blot

Transfected HEK293 cells were lysed in lysis buffer (50 mmol/L Tris, pH 7.4, 150 mmol/L NaCl, 1% Triton X-400, 1% sodium deoxycholate, 0.1% SDS and protein inhibitor) for 1 h. The cell extracts were then centrifuged for 30 min at 12 000 rpm at 4°C and supernatants were collected. The proteins were equally divided into three portions, and then separated by 4× sodium dodecyl sulfate (SDS) sample buffer with 200 mmol/L, 40 mmol/L, or no DTT. Approximately 20 µg of total protein from whole-cell extracts was loaded onto 10% non-reducing gel. Proteins were transferred to nitrocellulose filter membrane and probed with antibodies. Data were from four to five independent experiments.

### Detection of FRET Using Three-cube FRET Measurement

The fluorescence imaging work-station for FRET and the FRET quantification method have been described previously<sup>[4,11]</sup>. Briefly, the fluorescence imaging work-station consisted of a TE2000 inverted microscope (Nikon), Dual-View™ (Optical Insight) and a SNAP-HQ-cooled CCD (Roper Scientific). The FRET ratio (FR) was calculated with the following equation<sup>[14,15]</sup>:

$$FR = \frac{S_{FRET}(DA) - R_{D1} \cdot S_{CFP}(DA)}{R_{A1} \cdot S_{YFP}(DA)}$$

$S_{CUBE}$ (SPECIMEN) denotes an intensity measurement. CUBE indicates the filter cube, CFP, YFP or FRET, and SPECIMEN indicates the fluorescence from the cells expressing donor (D: CFP), acceptor (A; YFP), or both (DA).  $R_{D1}$  and  $R_{A1}$  were calculated to adjust the signals of donor and acceptor:  $R_{D1} = S_{FRET}(D)/S_{CFP}(D)$ ,  $R_{A1} = S_{FRET}(A)/S_{YFP}(A)$ .  $R_{D1}$  was calculated when the HEK293 cells expressed CFP only, and  $R_{A1}$  was calculated when the cells expressed YFP.

## RESULTS

### The ATD of the NMDAR GluN2A Subunit Spontaneously Forms Homodimers

In order to study the assembly of the GluN2A ATD, we linked the ATD to a transmembrane amino-acid sequence to ensure an endogenous environment for its translation and folding. We used the plasmid pDisplay which encodes a mouse Ig $\kappa$ -chain leader sequence to guide the target protein into the endoplasmic reticulum (ER). We made two constructs, pD-ATD<sub>2A</sub>-CFP and pD-ATD<sub>2A</sub>-YFP by inserting the GluN2A ATD into the C-terminus of the transmembrane domain of platelet-derived growth factor receptor (PDGFR) which was also encoded by pDisplay, and then adding a CFP or YFP between the leading sequence and the GluN2A ATD (Fig. 1A). This strategy has been widely used in previous studies<sup>[10,16]</sup>.

First, we used FRET to determine whether the GluN2A ATD could spontaneously form homodimers. We co-transfected CFP and YFP as the negative control, and the CFP-YFP chimera served as the positive control to ensure system reliability. The FRET values were  $1.16 \pm 0.03$  for CFP+YFP ( $n = 50$ ) and  $4.61 \pm 0.04$  for CFP-YFP ( $n = 43$ ) (Fig. 1B). Next, we evaluated the dimerization of the pDisplay transmembrane region by connecting a CFP or YFP to the N-terminal side of the pDisplay transmembrane region to construct pD-CFP and pD-YFP and then co-transfected these two chimeras into HEK293 cells for FRET detection. The FRET value was  $3.25 \pm 0.16$  for the pD-CFP and pD-YFP co-transfected group ( $n = 43$ ), which was lower than the pD-ATD<sub>2A</sub>-CFP and pD-ATD<sub>2A</sub>-YFP co-transfected group ( $6.14 \pm 0.5$ ,  $n = 59$ ) ( $P < 0.005$ ) (Fig. 1B). The FRET value of the pD-ATD<sub>2A</sub>-CFP and pD-ATD<sub>2A</sub>-YFP co-transfected group doubled that of the pD-CFP and pD-

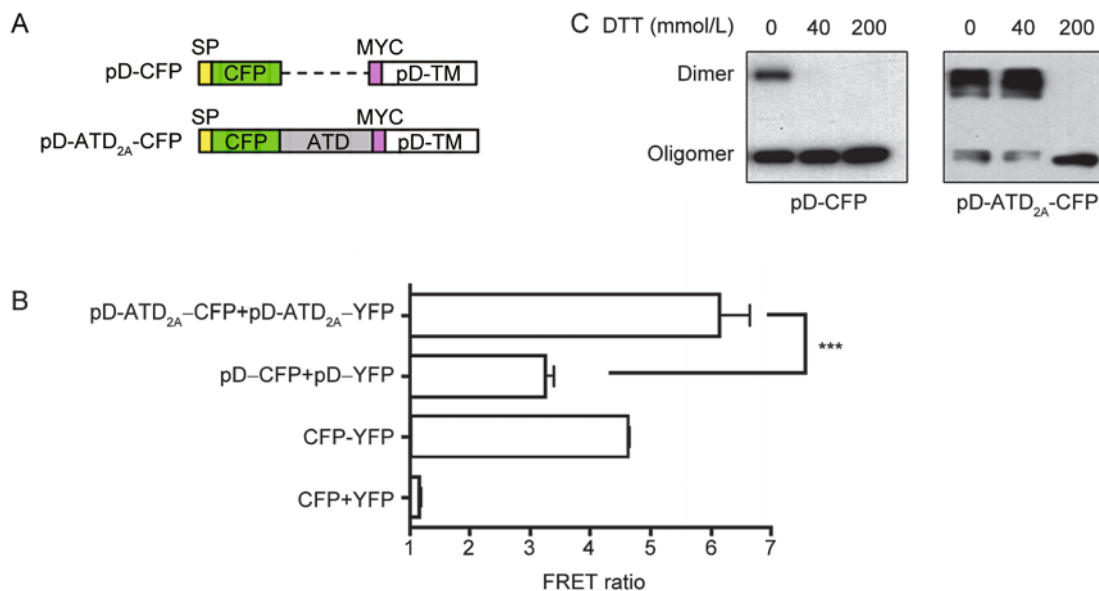


**Fig. 1.** The ATD of GluN2A forms homodimers. **A:** Schematic diagrams of pD-CFP/YFP and pD-ATD<sub>2A</sub>-CFP/YFP. Yellow boxes, mouse Ig $\kappa$ -chain leader sequence. Green bars, CFP or YFP. Gray bar, ATD of GluN2A. Pink boxes, myc tag. White bars, transmembrane domain of platelet-derived growth factor receptor. The leader sequence and transmembrane domain were encoded by plasmid p-Display. **B:** FRET analysis of interaction between pD-ATD<sub>2A</sub>-CFP/pD-ATD<sub>2A</sub>-YFP or pD-CFP/pD-YFP expressed in HEK293 cells. About 50 cells were measured. \*\*\* $P < 0.005$ . CFP+YFP stands for co-transfection of CFP and YFP, which served as negative control. CFP-YFP stands for a fusion protein of CFP and YFP with a short linker peptide, which served as positive control. Statistical analysis was by one-way ANOVA and statistical data are presented as mean  $\pm$  SEM. **C:** Detecting dimerization of pD-CFP and pD-ATD<sub>2A</sub>-CFP by non-reducing gel. The extracts of HEK293 cells transfected with pD-CFP or pD-ATD<sub>2A</sub>-CFP were divided equally into three parts, each was then dissolved in 4 $\times$  sample buffers containing 200 mmol/L or 40 mmol/L DTT or DTT-free sample buffer, and finally loaded onto 10% non-reducing gel. Data are from five independent experiments ( $n = 5$ ).

YFP co-transfected group, indicating that pD-ATD<sub>2A</sub>-CFP and pD-ATD<sub>2A</sub>-YFP interact more intimately, and GluN2A-ATD can dimerize and pull their transmembrane regions closer together.

To further confirm this result and determine whether the GluN2A ATD dimerization is mediated by disulfide bonds as in the GluN1 ATD, we transfected HEK293 cells with pD-CFP or pD-ATD<sub>2A</sub>-CFP, and harvested them 24 h later. Samples were subsequently subjected to non-reducing SDS-PAGE electrophoresis. Remarkably, nearly all the pD-CFP was detected as monomers and the pD-ATD<sub>2A</sub>-CFP as dimers, and pD-ATD<sub>2A</sub>-CFP was monomerized only in the presence of 200 mmol/L DTT (Fig. 1C). The dimerization of pD-ATD<sub>2A</sub> was further confirmed by co-immunoprecipitation (Co-IP) (Fig. 2B). The above results from FRET and non-reducing gel electrophoresis supported the conclusion that the ATD of GluN2A spontaneously forms homodimers *via*

disulfide bonds.

### Two Cysteine Residues Mediate Dimerization of the GluN2A ATD

Previous results have suggested that the GluN2A ATD spontaneously forms homodimers and that the dimerization is DTT-sensitive, indicating that it is reliant on disulfide bonds. So, next we set out to identify the specific cysteine residues responsible for this covalent binding. By aligning with leucine-, isoleucine-, and valine-binding proteins (LIVBPs) and the ATD of mGluRs, we found three cysteine residues, C87, C231 and C320 residing in the clamshell structure of the GluN2A-ATD. Each of these residues was separately substituted by alanine to generate the three mutations pD-ATD<sub>2A</sub>-C87A-CFP, pD-ATD<sub>2A</sub>-C231A-CFP, and pD-ATD<sub>2A</sub>-C320A-CFP. Then we used non-reducing gel electrophoresis to examine the formation of covalent

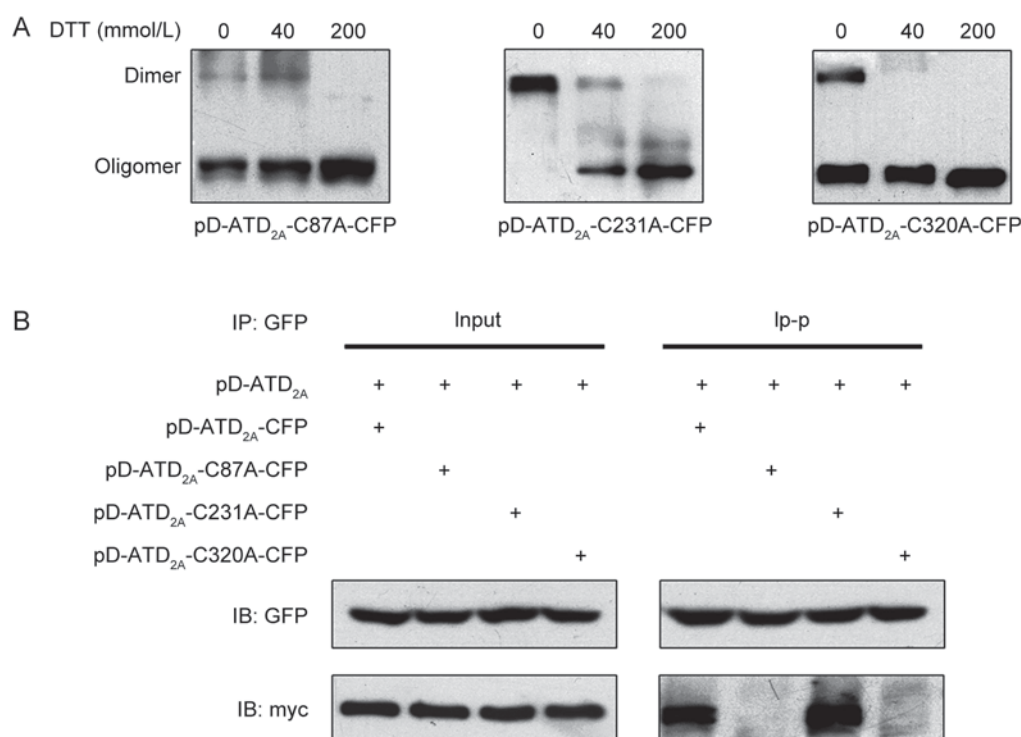


**Fig. 2.** Identification of two cysteine residues required for dimerization of the GluN2A ATD. **A:** Substituting cysteine 87 or cysteine 320 but not cysteine 231 of the GluN2A ATD with alanine abolished its homodimer formation. The single amino-acid-mutated pD-ATD<sub>2A</sub>-CFP was transfected into HEK293 cells, and non-reducing gel was used to assess the dimer formation ( $n = 4$ ). **B:** The interactions between pD-ATD<sub>2A</sub> and the three pD-ATD<sub>2A</sub>-CFP mutants shown by Co-IP. Rabbit anti-GFP antibody was used to precipitate pD-ATD<sub>2A</sub>-CFP, and GFP and myc antibodies were used to blot pD-ATD<sub>2A</sub>-CFP and pD-ATD<sub>2A</sub>, respectively. The pD-ATD<sub>2A</sub> and pD-ATD<sub>2A</sub>-CFP were recognized either by molecular weight or the different tag proteins they contained ( $n = 4$ ).

interactions by these mutants. Interestingly, we found that the C87A or the C320A mutation severely disrupted covalent binding. pD-ATD<sub>2A</sub>-C87A-CFP and pD-ATD<sub>2A</sub>-C320A-CFP mostly presented as monomers in DTT-free conditions. The C231A mutation, however, did not have a significant influence on the covalent binding of pD-ATD<sub>2A</sub>. This result suggested that both of these cysteine residues are required for the inter-subunit covalent binding of the GluN2A-ATD dimer, and mutation of either residue abolishes the disulfide binding (Fig. 2A).

Next, we continued to explore whether the formation of disulfide bonds is required for the homodimerization of the GluN2A subunit ATD. We co-transfected pD-ATD<sub>2A</sub>, which had no fluorescent protein attached to its N-terminus, with one of pD-ATD<sub>2A</sub>-C87A-CFP, pD-ATD<sub>2A</sub>-C231A-CFP or pD-ATD<sub>2A</sub>-C320A-CFP into HEK293 cells for Co-IP. The results showed that the pD-ATD<sub>2A</sub>-CFP with mutated C87A or C320A did not interact with pD-ATD<sub>2A</sub>, while pD-ATD<sub>2A</sub>-C231A-CFP still did so (Fig. 2B). In summary, the above experiments suggested that the formation of GluN2A-ATD homodimers is reliant on both cysteine residues, C87 and C320, without which the disulfide bonds cannot form and the homodimer cannot assemble.

### The Monomer of the GluN2A Subunit ATD Can Form a Heterodimer with the GluN1 ATD

In order to investigate whether monomer pD-ATD<sub>2A</sub>-C87A-CFP or pD-ATD<sub>2A</sub>-C320A-CFP still assembles with the GluN1 ATD, we constructed pD-ATD<sub>GluN1</sub> using the same strategy as with pD-ATD<sub>2A</sub>, and co-transfected the three GluN2A ATD mutants pD-ATD<sub>2A</sub>-C87A-CFP, pD-ATD<sub>2A</sub>-C231A-CFP and pD-ATD<sub>2A</sub>-C320A-CFP, or pD-ATD<sub>2A</sub>-CFP with pD-ATD<sub>GluN1</sub> into HEK293 cells. Then we used polyclonal GFP antibodies for Co-IP, and found that among the four co-transfected groups, all three mutated GluN2A ATDs precipitated the GluN1 ATD which indicated that GluN2A-ATD dimerization is not a prerequisite for the interaction of the GluN2A and GluN1 ATDs (Fig. 3A).

Next, we attempted to confirm our findings by cell imaging. Our previous study indicated that the GluN2A ATD contains a specific ER retention signal that can be masked by GluN1 during assembly<sup>[10]</sup>. Thus we investigated whether mutant GluN2A ATDs translocated to the plasma membrane with the assistance of the GluN1 ATD. We first determined whether the point mutation would destroy the

ER retention of the GluN2A ATD. We transfected pD-ATD<sub>2A</sub>-CFP, pD-ATD<sub>2A</sub>-C87A-CFP, pD-ATD<sub>2A</sub>-C231A-CFP, pD-ATD<sub>2A</sub>-C320A-CFP or positive control pD-CFP into COS-7 cells and performed surface staining with GFP antibodies. Because CFP was connected to the extracellular N-terminus of the chimera protein, red clusters were seen if the chimera proteins were successfully expressed on the cell surface. As expected, we found that in the pD-CFP-transfected COS-7 cells, intense red fluorescence was present on the cell surface. However, neither HEK293 cells transfected with pD-ATD<sub>2A</sub>-CFP nor its mutant types emitted a surface-staining signal (Fig. 3B). Therefore the 2A-ATD cysteine mutation was not sufficient to overcome ER retention. We further confirmed this result by investigating the subcellular localization of pD-ATD<sub>2A</sub>-CFP and the three mutants using calreticulin as the ER marker. We found that all the mutants significantly co-localized with calreticulin (Fig. 3C). These results showed that mutations of these three cysteine residues have no influence on ER retention of the GluN2A ATD.

Next, we co-transfected pD-ATD<sub>GluN1</sub> with pD-ATD<sub>2A</sub>-CFP, pD-ATD<sub>2A</sub>-C87A-CFP, pD-ATD<sub>2A</sub>-C231A-CFP or pD-ATD<sub>2A</sub>-C320A-CFP, and intense fluorescent staining was detected on the cell surface of all four groups, suggesting that the three GluN2A-ATD mutants were exported from the ER and translocated to the plasma membrane with the assistance of the GluN1 ATD (Fig. 4A). Statistics showed that in the pD-ATD<sub>2A</sub>-CFP and pD-ATD<sub>GluN1</sub> co-transfected group,  $56.6 \pm 3.3\%$  ( $n = 6$ ) of the successfully-transfected cells had positive surface labeling. When pD-ATD<sub>GluN1</sub> was co-transfected with the three GluN2A-ATD mutants, comparable percentages of positive surface-labeled cells were detected [ $56.3 \pm 3.8\%$  ( $n = 6$ ) for pD-ATD<sub>2A</sub>-C87A-CFP,  $49.2 \pm 4.0\%$  ( $n = 6$ ) for pD-ATD<sub>2A</sub>-C231A-CFP, and  $45.9 \pm 4.6\%$  ( $n = 6$ ) for pD-ATD<sub>2A</sub>-C87A-CFP]. But in the pD-ATD<sub>2A</sub>-CFP single-transfected group, few cells ( $1.8 \pm 0.7\%$ ,  $n = 6$ ) had surface labeling (Fig. 4B). The above results indicated that the GluN2A-ATD monomer can assemble into heterodimers with the GluN1 ATD, and dimerization of the Glu2A ATD is not required for the GluN2A-ATD and GluN1-ATD interaction.

### Dimerization of GluN2A Is Dependent on Two Cysteine Residues in the ATD

We first investigated the dimerization of endogenous

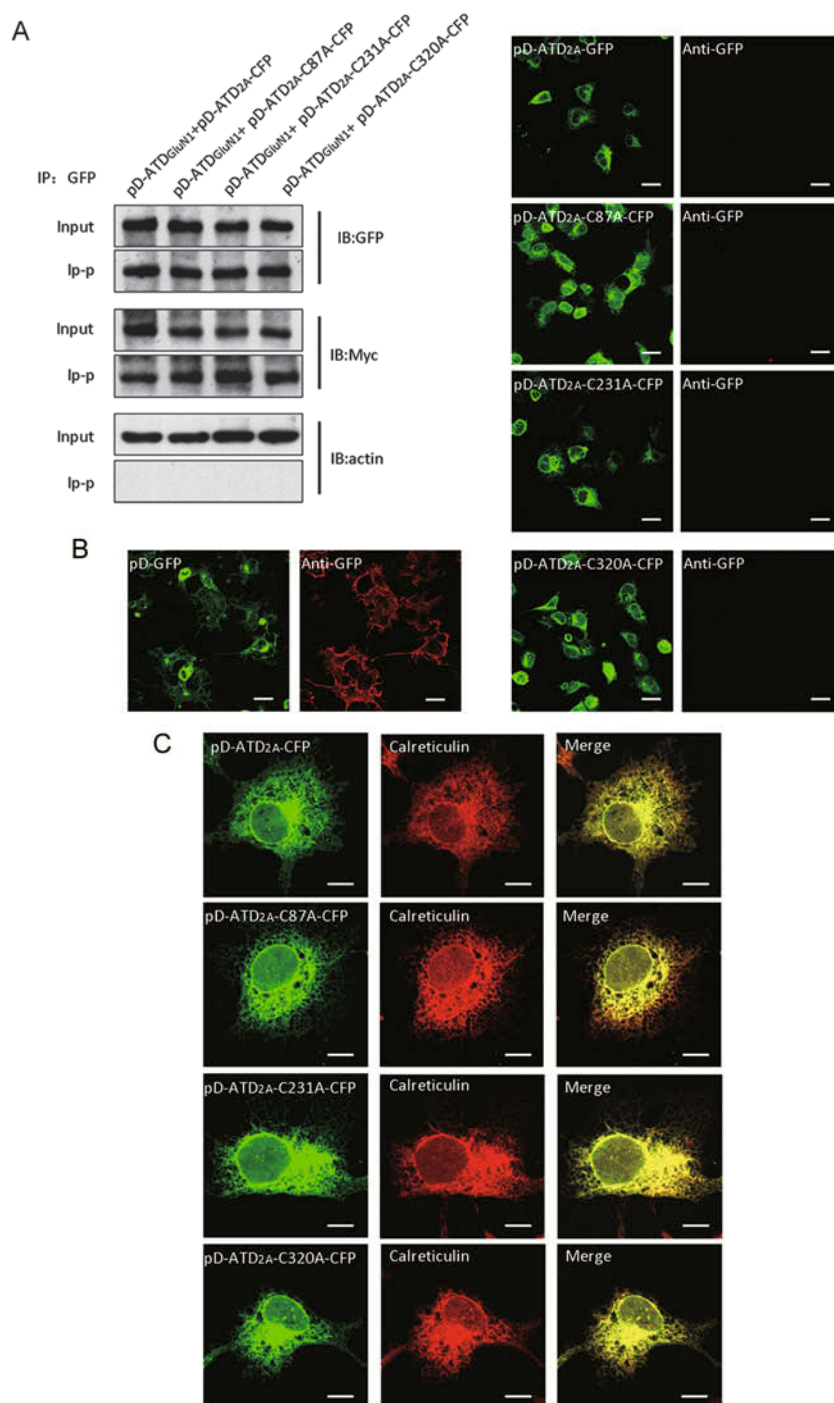


**Fig. 3.** Cysteine mutations do not hinder the interaction between the GluN2A and GluN1 ATDs or destroy the ER retention signal located in the ATD of GluN2A. **A:** The interactions between pD-ATD2A-CFP or the three pD-ATD2A-CFP mutants and pD-ATDGluN1 were assessed by Co-IP. The proteins were expressed in HEK293 cells. Actin served as a negative control ( $n = 4$ ). **B:** The surface expression of the three pD-ATD2A-CFP mutants was detected in HEK293 cells. pD-CFP served as positive control. The surface-expressed proteins were labeled red by rabbit anti-GFP primary antibody and Alexa546-conjugated secondary antibody under non-permeable conditions because the GFP tag was attached to the extracellular side of the transmembrane domain. Scale bar, 10  $\mu\text{m}$ . **C:** Subcellular localization of the three mutants: pD-ATD2A-C87A-CFP, pD-ATD2A-C231A-CFP, and pD-ATD2A-C320A-CFP. Cysteine-mutated pD-ATD2A-CFP still had a fine co-localization with the ER marker calreticulin. Green indicates pD-ATD2A-CFP, and red indicates calreticulin. Scale bars, 5  $\mu\text{m}$ .

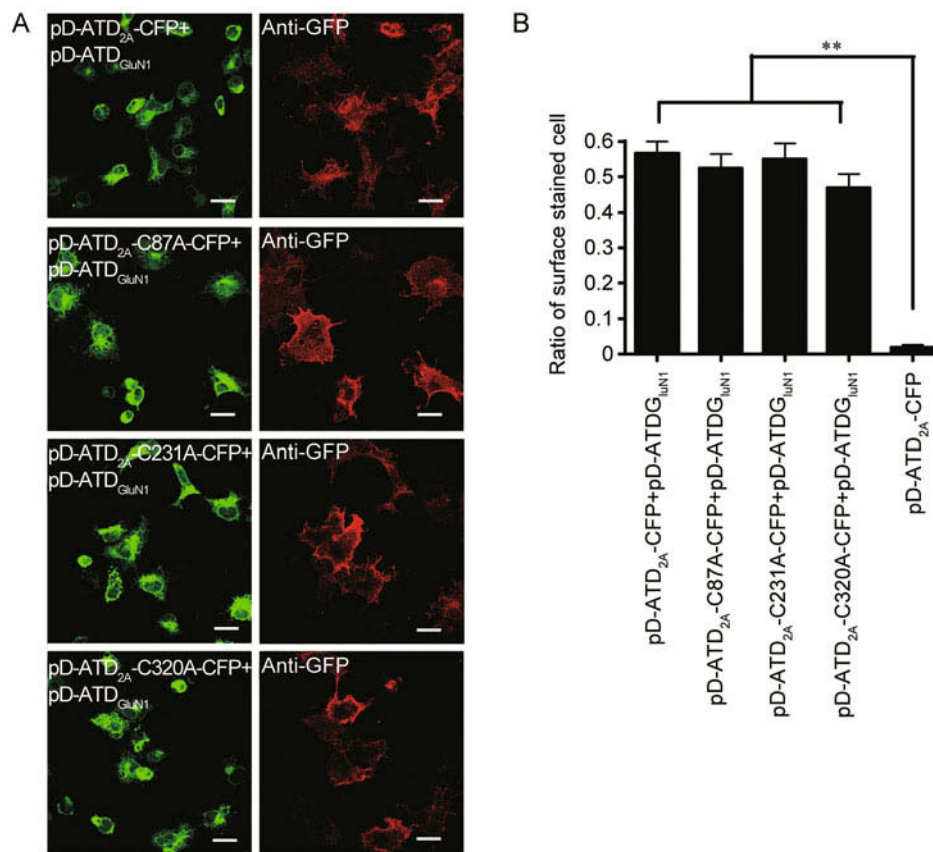


**Fig. 4.** The formation of homodimers by the GluN2A ATD is not required for its assembly with the GluN1 ATD. **A:** Co-transfection of pD-ATD<sub>GluN1</sub> with wild-type or the three mutants of pD-ATD<sub>2A</sub>-CFP in HEK293 cells. The surface-staining indicates that the monomer-forming pD-ATD<sub>2A</sub>-C87A-CFP and pD-ATD<sub>2A</sub>-C320A-CFP are able to assemble with pD-ATD<sub>GluN1</sub> and are expressed on the cell membrane. Scale bars, 10  $\mu$ m. **B:** Statistical data from six independent experiments showing the percentages of HEK293 cells with positive surface labeling. \*\* $P < 0.01$ . More than 300 cells were analyzed. Mean  $\pm$  SEM, one-way ANOVA.

GluN2A in rat cortex, and found that under non-reducing conditions, nearly all GluN2A subunits were present as dimers. The dimers were stable in 40 mmol/L DTT, and were only monomerized when the DTT concentration reached 200 mmol/L (Fig. 5A). We further confirmed that GluN2A subunits form homodimers using heterogeneous expression systems. GluN2A-CFP was transfected into HEK293 cells, and again GluN2A-CFP dimers were detected (Fig. 5B). The dimers were surprisingly stable, as 200 mmol/L DTT was insufficient to break the interaction between subunit pairs, which may be due to overexpression of the target protein in the transfection system.

So far, we have demonstrated that both endogenous and heterogeneous GluN2A form dimers by covalent interaction. We constructed the three cysteine mutants

GluN2A-C87A-CFP, GluN2A-C231A-CFP, and GluN2A-C320A-CFP on the basis of GluN2A-CFP and found that when expressed alone in HEK293 cells, GluN2A-C87A-CFP and GluN2A-C320A-CFP were in monomer form, while GluN2A-C231A-GFP remained a homodimer (Fig. 5C). This indicated that GluN2A-CFP can indeed form dimers, and the homogenous GluN2A dimers detected earlier were not the result of membrane protein aggregation, but were due to the formation of disulfide bonds. Moreover, this suggested that only two pairs of cysteine residues (C87 and C320) of the GluN2A ATD can form disulfide bonds, or these two residues are of primary importance for the formation of other disulfide bonds. As a result, mutation of either of these residues would abolish GluN2A dimerization. In summary, GluN2A exists as dimers under

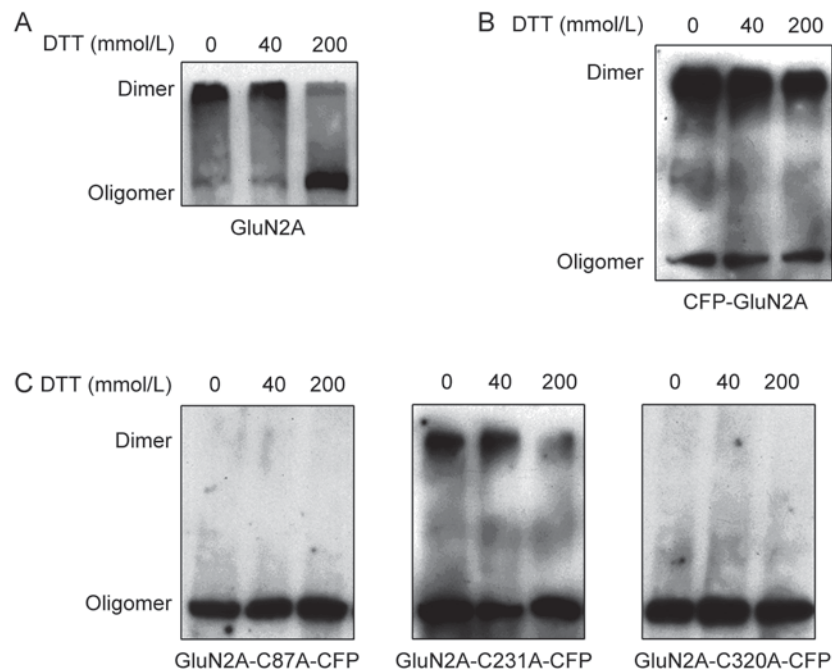


**Fig. 5.** The homodimerization of full-length GluN2A depends on two cysteines in the ATD of GluN2A. **A:** Protein samples of adult rat cortex dissolved in buffers containing different concentrations of DTT were loaded onto non-reducing gel to assess homodimers of GluN2A ( $n = 4$ ). **B:** The homodimer of GluN2A-CFP was investigated in HEK293 cells. GluN2A-GFP was transfected into HEK293 cells, and homodimer formation was examined by non-reducing gel ( $n = 4$ ). **C:** GluN2A-C87A-GFP, GluN2A-C231A-GFP, or GluN2A-C320A-GFP was transfected into HEK293 cells. GluN2A-C87A-GFP and GluN2A-C320A-GFP were present as monomers on non-reducing gel ( $n = 4$ ).

physiological conditions, and the two pairs of cysteine residues responsible for inter-subunit disulfide bonding are located in the ATD region.

#### GluN2A ATD Dimerization Is Not Required for the Interaction of GluN2A and GluN1

Early studies discovered that the C79 residue of GluN1 mediates GluN1 dimerization, and is essential for GluN1 and GluN2A interactions as well as surface expression in the plasma membrane<sup>[5]</sup>. Therefore, we investigated whether the C87- and C320-dependent GluN2A-ATD dimerization is necessary for GluN2A and GluN1 assembly and surface expression.

We co-transfected GluN2A-CFP, GluN2A-C87A-CFP, GluN2A-C231A-CFP or GluN2A-C320A-CFP with wild-type GluN1 (wt-GluN1) for Co-IP and discovered that GluN2A efficiently precipitated GluN1 in all four transfection groups, which indicated that the C87A and C320A mutations did not disrupt GluN2A and GluN1 assembly, implying that GluN2A

ATD dimerization had no influence on the assembly of GluN2A with GluN1 (Fig. 6A). To further confirm our results, we examined the surface expression of wild-type and mutated GluN2A co-transfected with wt-GluN1. The four combinations of GluN2A-CFP/wt-GluN1, GluN2A-C87A-CFP/wt-GluN1, GluN2A-C231A-CFP/wt-GluN1, and GluN2A-C320A-CFP/wt-GluN1 were co-transfected into COS-7 cells. Consistent with our previous biochemical experiments, we found that all three GluN2A mutants were detected on the cell surface (Fig. 6B), suggesting that GluN2A indeed assembles with GluN1 into a mature tetramer and is expressed on the cell membrane. Finally, we transfected GluN2A-C87A-CFP, GluN2A-C231A-CFP, GluN2A-C320A-CFP or GluN2A-CFP alone into cultured cortical neurons to see whether they assembled with endogenous GluN1 for surface expression. Positive surface labeling was seen for all three transfections (Fig. 6C). Altogether, the above experiments suggested that even if the GluN2A ATD did not dimerize, GluN2A and GluN1

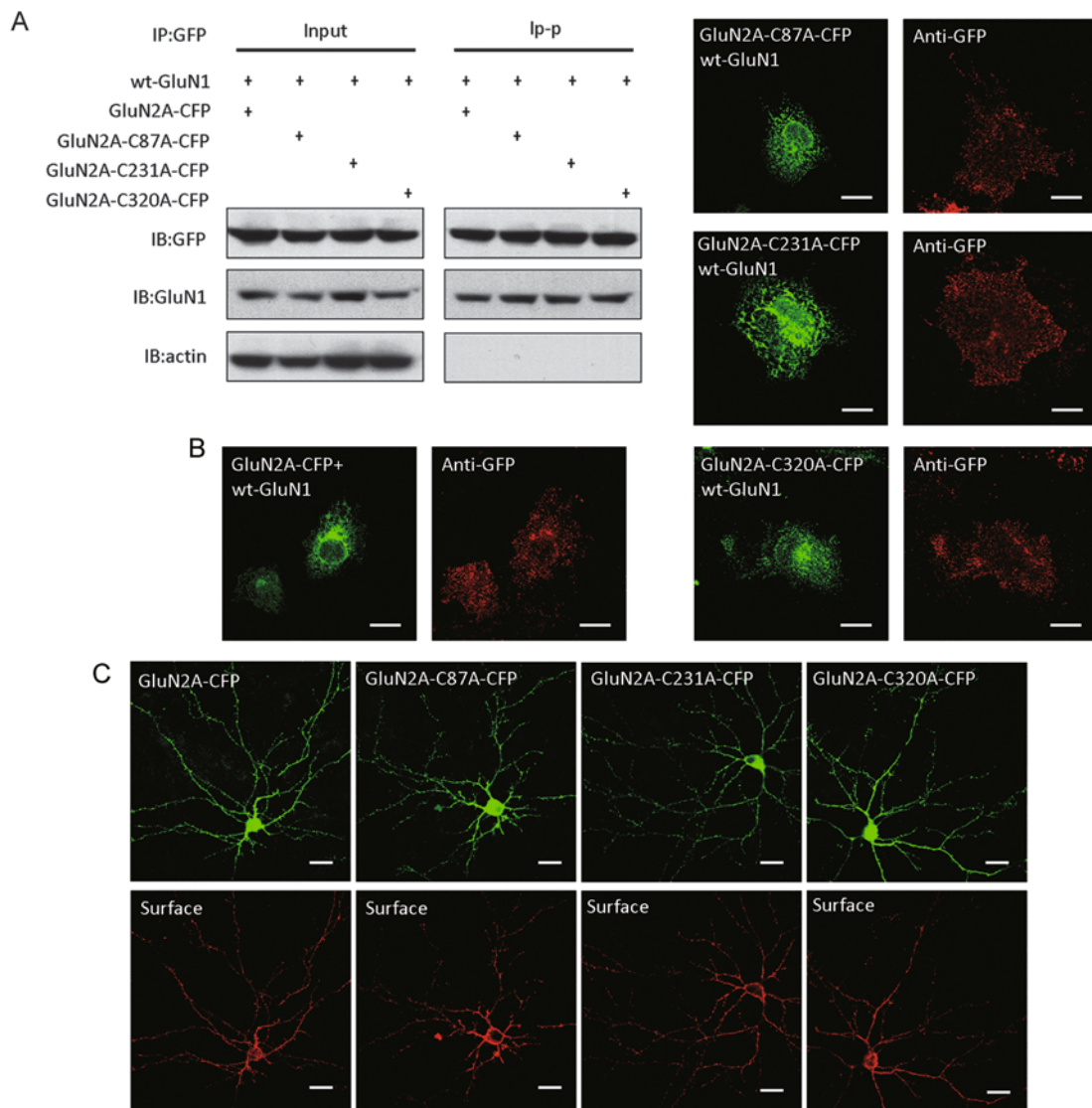


**Fig. 6. Homomerization of the GluN2A ATD is not a core step in NMDAR assembly.** **A:** Co-transfection of wild-type (wt)-GluN1 with GluN2A-CFP or the three mutated GluN2A-CFPs into HEK293 cells. Co-IP was used to assess the interaction of protein pairs in each group. GFP and GluN1 antibodies were used to blot GluN2A and GluN1 respectively, and actin served as a negative control ( $n = 4$ ). **B:** The same transfection combination as the Co-IP experiment was used, and the surface expression of mutated GluN2A was detected by labeling the extracellular GFP tag in the N-terminus of GluN2A with anti-GFP antibody and Alexa546-conjugated secondary antibody. Green indicates the total expression of GluN2A-CFP, and red clusters indicate the surface-expressed GluN2A. Scale bars, 10  $\mu$ m. **C:** GluN2A-CFP, GluN2A-C87A-CFP, GluN2A-C231A-CFP or GluN2A-C320A-CFP was expressed in cultured cortical neurons. The neurons were transfected on 10 days *in vitro* (DIV10) and immunostained on DIV14. Green indicates the total expression of GluN2A-CFP, and red indicates surface expression. Scale bars, 10  $\mu$ m.

assembly appeared not to be disrupted. So, based on our final result, the ATDs of GluN2A and GluN1 play different roles in NMDAR assembly, with dimerization of the GluN1 ATD being required for assembly while that of the GluN2A ATD being not.

## DISCUSSION

In this study, we investigated the role of the GluN2A amino terminal domain on the assembly of NMDARs. Combining FRET, biochemistry and Co-IP, we found that

two GluN2A ATDs formed a homodimer through the inter-subunit disulfide bonds of cysteine residues C87 and C320. Mutation of either of these residues disrupted GluN2A-ATD dimerization, irrespective of whether the ATD alone or full-length GluN2A was under study. It is accepted that the ATD of GluN1 also undergoes cysteine-dependent dimerization. Mutation of cysteine C79 disrupts GluN1 dimerization and decreases the surface expression of NMDARs<sup>[5]</sup>. Interestingly, in this study we found that the mutated GluN2A ATD, which itself cannot dimerize, was still capable of heterogeneous assembly with GluN1, nor did this affect the surface expression of the assembled receptors. Therefore, these results suggested that the ATDs of GluN1 and GluN2A play different roles in NMDAR assembly, and the GluN2A ATD does not initialize receptor assembly.

### The Functional Importance of ATD in Assembly of Glutamate Receptors

The N-terminal LIVBP-like domain, ATD, is located immediately downstream of the signal peptide, which is the first to be translated in each ionotropic glutamate receptor, so it may be a critical point for receptor assembly. Extensive research has shown that the N-terminus of AMPARs dimerizes when it is expressed alone in a heterogeneous system<sup>[17,18]</sup>. This dimerization is considered to be of major importance in the two-step assembly of AMPARs. Dimerization of the ATD is the starting-point for monomers to form dimers<sup>[19,20]</sup>. Dimers then further assemble into tetramers as a result of multiple interaction sites on the subunits<sup>[21]</sup>.

The NMDAR ATD however, seems to work in a quite different way. A series of experiments was conducted to elucidate the function of different regions in subunit assembly using various truncations. Early studies showed that ATD-truncated GluN1 cannot complete assembly with GluN2A, and surface expression cannot be detected in HEK293 cells co-transfected with ATD-truncated GluN1 and wild-type GluN2A<sup>[22]</sup>. These results were confirmed by later studies which showed that ATD-truncated GluN1 and GluN2A are not expressed on the plasma membrane when co-expressed in heterogeneous systems. However, others argue that this is because the GluN2A ATD contains an ER-specific retention signal and is not due to a defect of assembly<sup>[10]</sup>. In addition, evidence from FRET assays also showed that homodimeric or heterodimeric assembly

is not affected by either ATD-deleted GluN1 or ATD-deleted GluN2A/GluN2B<sup>[4, 11]</sup>. Moreover, the authors believe that the discrepancy is due to the higher sensitivity of FRET over Co-IP, and the latter is conducted in a more endogenous environment.

Other evidence comes from studies aimed at exploring the behavior of the separated NMDAR ATD or the subunits as a whole. The ATDs of the NMDAR GluN1 and GluN2B subunits are present as monomers when expressed alone, which is different from other glutamatergic receptor ATDs that are capable of forming stable dimers<sup>[23,24]</sup>. This result suggests that during NMDAR subunit assembly, the first translated ATD is not able to pull together the remaining components of the NMDAR. Thus, the ATD of NMDARs is unlikely to be a core domain of assembly. Our results strongly support this, as the introduction of mutations at C87 and C320 in the GluN2A ATD hindered the dimerization of GluN2A, but the receptor still assembled successfully. Although research has shown that the C79 residue mediates a disulfide bond in the GluN1 ATD and is crucial for maintaining the assembly of dimerized GluN1 and GluN2, combining the result that heterogeneously-expressed GluN1 ATD is present as monomer and the fact that the transmembrane region of NMDARs can form dimers, it may be that the disulfide bond between ATDs is established after receptor assembly, and functions to stabilize the receptor instead of being the beginning of assembly.

### The Subunit Arrangement of NMDARs

Since the complete crystallized structure of NMDAR subunits has not yet been identified, no direct evidence describes the spatial organization of subunits after NMDAR assembly. The study of the arrangement of NMDAR subunits is currently carried out by two types of experimental approaches. First, sequence alignment of AMPARs and NMDARs to predict possible modes of NMDAR assembly and verification by biochemical assays. Second, partial crystallization analysis of NMDAR fragments. Investigation of AMPAR structure has found that it can be divided into three parts: the 4-fold symmetrical transmembrane region and the 2-fold symmetrical ligand-binding domain (LBD), and the ATD. The relative locations of these three parts of four subunits has not reached consensus. In the 2-fold symmetrical LBD and ATD,

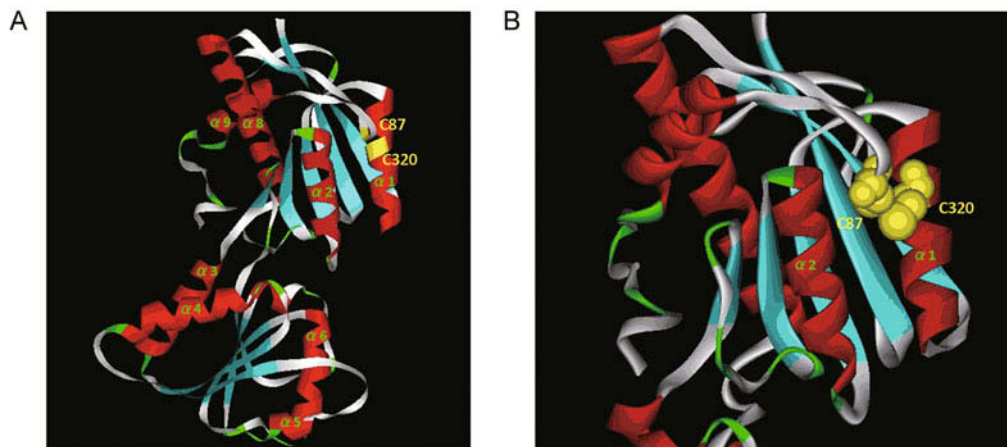


**Fig. 7. Model for the location of C87 and C320. A and B:** Simulated structure of the GluN2A ATD based on GluN2B. Red ribbons indicate  $\alpha$ -helices. Light-blue ribbons indicate  $\beta$ -sheets. Yellow segments indicate C87 or C320. C87 and C320 are both located on the surface of the R1 subdomain of the GluN2A ATD.

two of the four subunits lie close to each other and are called B and D, while the other two subunits, A and C, are relatively far apart. By simulating an NMDAR based on AMPA structure, the GluN1 LBD was identified as proximal, because GluN1 P661C can crosslink GluN1 under non-reducing conditions. GluN2A does not contain such sites for cross-linking<sup>[25]</sup>. In later research combining cysteine mutation with electrophysiological assay, GluN1 was determined as the proximal subunit both in the NMDAR transmembrane region and the LBD<sup>[7]</sup>.

However, crystallization analysis of the GluN2B and GluN1 ATDs shows structural characteristics slightly different from the AMPAR ATD. When aligned and superimposed on the ATDs of AMPA and kainate receptors, the R1 and R2 subdomains of the GluN1 and GluN2B ATDs are rotated by 45–50° relative to each other. This allows the two GluN2B ATDs to be anchored at a proximal position, while the two GluN1 ATDs are in a distal position<sup>[23,24]</sup>. Our research is consistent with this model, as we found that all endogenous GluN2A formed homodimers *via* two cysteine residues in the ATDs. Besides, we built a three-dimensional homology model of the GluN2A ATD based on GluN2B-ATD structure (PDB ID: 3jpw)<sup>[23]</sup> using the SWISS-MODEL workspace (<http://swissmodel.expasy.org/>)<sup>[26]</sup>. As shown in Fig. 7, C87 is located in helix 1 and C320 in a loop between helices 8 and 9. And both C87 and C320 are on the surface of the R1 subdomain of the GluN2A ATD, while C231 is not, which is in accord with the former experimental results.

And these two residues are adjacent to each other, which indicates the interface between two GluN2A ATDs (Fig. 7). Since most GluN2A subunits exist as fully-assembled hetero-tetramers, the formation of disulfide bonds between GluN2A ATDs suggests that they represent the proximal B and D position.

#### Reconfiguration of Subunits during Assembly

So far, NMDAR assembly may be much more complicated than that of AMPARs. Much evidence shows that NMDARs assemble asymmetrically. GluN1 subunits first form dimers, and then assemble with different kinds of GluN2 subunits to form heterotetramers<sup>[27]</sup>. Assembly is completed with the LBDs of two GluN1s and the ATDs of GluN2s in proximal positions. However, early studies have shown that the GluN1 ATD carries a cysteine residue for disulfide bonding, which is essential for receptor assembly<sup>[5]</sup>. Moreover, heterogeneously-expressed GluN2 subunits exist as dimers. Our studies also demonstrated that GluN2A subunit homomerization was mediated by cysteine residues C87 and C320 in the ATD region. But how can the GluN1 ATDs be in distal positions if they mediate disulfide binding? Recent studies argue that NMDARs undergo reconfiguration during tetramer formation, with the disulfide bond of GluN1 being deoxidized during assembly with GluN2. And mandatory cross-linking of GluN1 subunits hinders GluN2 assembly<sup>[24]</sup>. Early FRET studies have shown that GluN2 exhibits a higher FRET value in

tetramers than in homodimers. This indicates that the interaction between GluN2s is weak, and is competitively replaced by heterogeneous subunit interactions during tetramer assembly, which eventually reconfigure into the final tetramer<sup>[4]</sup>. This process can be verified in future studies, because we have identified the specific cysteine residues necessary for GluN2-ATD dimerization; it will be interesting to investigate whether reconfiguration occurs in GluN2 assembly as in GluN1.

The various types and diverse combinations of NMDAR subunits determine the specific function of different NMDARs. As NMDAR expression is regulated by synaptic activity, a comprehensive understanding of NMDARs is crucial for further functional investigations.

#### ACKNOWLEDGEMENTS

This work was supported by grants from the National Basic Research Development Program of China (2010CB912002) and the National Natural Science Foundation of China (30730038 and 81171164).

Received date: 2012-10-09; Accepted date: 2012-11-15

#### REFERENCES

- [1] Meguro H, Mori H, Araki K, Kushiya E, Kutsuwada T, Yamazaki M, *et al.* Functional characterization of a heteromeric NMDA receptor channel expressed from cloned cDNAs. *Nature* 1992, 357: 70–74.
- [2] Monyer H, Sprengel R, Schoepfer R, Herb A, Higuchi M, Lomeli H, *et al.* Heteromeric NMDA receptors: molecular and functional distinction of subtypes. *Science* 1992, 256: 1217–1221.
- [3] Schorge S, Colquhoun D. Studies of NMDA receptor function and stoichiometry with truncated and tandem subunits. *J Neurosci* 2003, 23: 1151–1158.
- [4] Qiu S, Hua YL, Yang F, Chen YZ, Luo JH. Subunit assembly of N-methyl-d-aspartate receptors analyzed by fluorescence resonance energy transfer. *J Biol Chem* 2005, 280: 24923–24930.
- [5] Papadakis M, Hawkins LM, Stephenson FA. Appropriate NR1-NR1 disulfide-linked homodimer formation is requisite for efficient expression of functional, cell surface N-methyl-D-aspartate NR1/NR2 receptors. *J Biol Chem* 2004, 279: 14703–14712.
- [6] Lee CH, Gouaux E. Amino terminal domains of the NMDA receptor are organized as local heterodimers. *PLoS One* 2011, 6: e19180.
- [7] Riou M, Stroebel D, Edwardson JM, Paoletti P. An alternating GluN1-2-1-2 subunit arrangement in mature NMDA receptors. *PLoS One* 2012, 7: e35134.
- [8] Furukawa H, Singh SK, Mancusso R, Gouaux E. Subunit arrangement and function in NMDA receptors. *Nature* 2005, 438: 185–192.
- [9] Kumar J, Schuck P, Mayer ML. Structure and assembly mechanism for heteromeric kainate receptors. *Neuron* 2011, 71: 319–331.
- [10] Qiu S, Zhang XM, Cao JY, Yang W, Yan YG, Shan L, *et al.* An endoplasmic reticulum retention signal located in the extracellular amino-terminal domain of the NR2A subunit of N-methyl-d-aspartate receptors. *J Biol Chem* 2009, 284: 20285–20298.
- [11] Cao JY, Qiu S, Zhang J, Wang JJ, Zhang XM, Luo JH. Transmembrane region of N-methyl-d-aspartate receptor (NMDAR) subunit is required for receptor subunit assembly. *J Biol Chem* 2011, 286: 27698–27705.
- [12] Luo JH, Fu ZY, Losi G, Kim BG, Prybylowski K, Vissel B, *et al.* Functional expression of distinct NMDA channel subunits tagged with green fluorescent protein in hippocampal neurons in culture. *Neuropharmacology* 2002, 42: 306–318.
- [13] Yang W, Zheng C, Song Q, Yang X, Qiu S, Liu C, *et al.* A Three amino acid tail following the TM4 region of the N-methyl-D-aspartate receptor (NR) 2 subunits is sufficient to overcome endoplasmic reticulum retention of NR1-1a subunit. *J Biol Chem* 2007, 282: 9269–9278.
- [14] Erickson MG, Alseikhan BA, Peterson BZ, Yue DT. Preassociation of calmodulin with voltage-gated Ca<sup>2+</sup> channels revealed by FRET in single living cells. *Neuron* 2001, 31: 973–985.
- [15] Erickson MG, Liang H, Mori MX, Yue DT. FRET two-hybrid mapping reveals function and location of L-type Ca<sup>2+</sup> channel CaM preassociation. *Neuron* 2003, 39: 97–107.
- [16] Saglietti L, Dequidt C, Kamieniarz K, Rousset M-C, Valnegri P, Thoumine O, *et al.* Extracellular interactions between GluR2 and N-cadherin in spine regulation. *Neuron* 2007, 54: 461–477.
- [17] Kuusinen A, Abele R, Madden DR, Keinänen K. Oligomerization and ligand-binding properties of the ectodomain of the  $\alpha$ -amino-3-hydroxy-5-methyl-4-isoxazole propionic acid receptor subunit GluRD. *J Biol Chem* 1999, 274: 28937–28943.
- [18] Wells GB, Lin L, Jeanclous EM, Anand R. Assembly and ligand binding properties of the water-soluble extracellular domains of the glutamate receptor 1 subunit. *J Biol Chem* 2001, 276: 3031–3036.
- [19] Jin R, Singh SK, Gu S, Furukawa H, Sobolevsky AI, Zhou J, *et al.* Crystal structure and association behaviour of the GluR2 amino-terminal domain. *EMBO J* 2009, 28: 1812–

- 1823.
- [20] Ayalon G, Segev E, Elgavish S, Stern-Bach Y. Two regions in the N-terminal domain of ionotropic glutamate receptor 3 form the subunit oligomerization interfaces that control subtype-specific receptor assembly. *J Biol Chem* 2005, 280: 15053–15060.
- [21] Ayalon G, Stern-Bach Y. Functional assembly of AMPA and kainate receptors is mediated by several discrete protein-protein interactions. *Neuron* 2001, 31: 103–113.
- [22] Meddows E, Le Bourdellès B, Grimwood S, Wafford K, Sandhu S, Whiting P, *et al.* Identification of molecular determinants that are important in the assembly of N-methyl-d-aspartate receptors. *J Biol Chem* 2001, 276: 18795–18803.
- [23] Karakas E, Simorowski N, Furukawa H. Structure of the zinc-bound amino-terminal domain of the NMDA receptor NR2B subunit. *EMBO J* 2009, 28: 3910–3920.
- [24] Farina AN, Blain KY, Maruo T, Kwiatkowski W, Choe S, Nakagawa T. Separation of domain contacts is required for heterotetrameric assembly of functional NMDA receptors. *J Neurosci* 2011, 31: 3565–3579.
- [25] Sobolevsky AI, Rosconi MP, Gouaux E. X-ray structure, symmetry and mechanism of an AMPA-subtype glutamate receptor. *Nature* 2009, 462: 745–756.
- [26] Bordoli L, Kiefer F, Arnold K, Benkert P, Battey J, Schwede T. Protein structure homology modeling using SWISS-MODEL workspace. *Nat Protocols* 2008, 4: 1–13.
- [27] Atlason PT, Garside ML, Meddows E, Whiting P, McIlhinney RA. N-methyl-d-aspartate (NMDA) receptor subunit NR1 forms the substrate for oligomeric assembly of the NMDA receptor. *J Biol Chem* 2007, 282: 25299–25307.